tiferromagnetic interaction is negligible, and the temperature is low enough for the singlet states not to be significantly populated. Above 105 K, $\mu_{eff}$ decreases steadily on increasing the temperature up to 300 K due to the thermal population of the singlet states. The existence of some kind of weak inter- or/and intramolecular antiferromagnetic interactions is supported by a slight deviation of the magnetization at low temperatures (5 K) (see inset in Figure 2) from the expected behavior (eq 3) for a pair of independent triplet states separated from the excited singlet states by the energy gap $2J$:

$$M(T,H) = \frac{2FN_A}{A}\frac{\sum m_i e^{-E_i/k_BT}}{\sum e^{-E_i/k_BT}}$$

i.e.

$$M(T,H) = 2F\frac{N_A\mu_B g}{A}\frac{-e^{-2\mu_B H/k_BT} + e^{2\mu_B H/k_BT}}{e^{-2\mu_B H/k_BT} + e^{2\mu_B H/k_BT} + e^{-2J/k_BT} + 1} \quad (3)$$

where $m_i$ and $E_i$ are the magnetization and energy of each state, respectively, $N_A$ is the Avogadro's number, $A$ is the molecular weight, 2 is a factor due to the fact that two pairs of radical centers are present in the molecule, and $H$ is the magnitude of the applied magnetic field. Equation 3 represents the mean value of the magnetization per mass unit taking into account the thermal population of the triplet and singlet states of each pair of radical centers.

The $\Delta m_s = \pm 1$ region of the EPR spectrum of the sample obtained of **1** in frozen MTHF over the range 4-129 K shows a complex pattern with several lines (Figure 3), and some of these might be due to the presence of two diastereoisomeric forms of the molecule because of the restricted rotation of pentachlorophenyl groups.[12] Supporting the presence of these species, the $\Delta m_s = \pm 2$ region of the spectrum (Figure 3) exhibits two overlapping lines, one of which can be saturated by increasing the microwave power. From the two symmetric and outermost pairs of peaks with $\Delta m_s = \pm 1$, the zero splitting parameters $|D/hc|$ for these high-spin species are predicted to be 0.010 and 0.013 $cm^{-1}$. Such small values are in satisfactory agreement with those reported for *m*-xylylene (0.011 $cm^{-1}$)[13] and the two diastereoisomers of perchloro-*m*-xylylene (0.0156 and 0.0080 $cm^{-1}$).[14] The center peak of the spectrum is assigned to doublet impurities. Accordingly to this, the EPR spectrum of **1** in MTHF solution at room temperature seems to be a superposition of a sharp line and a broad line. The former, which has the characteristics ($g$ = 2.0033; $\Delta H_{pp}$ = 3.87 G) of the highly chlorinated triphenylmethyl radicals,[3] is attributed to the impurities.

Since it has been calculated that the triplet-singlet energy gap value is quite high (0.69 kcal/mol) and the signal intensity of the $\Delta m_s = \pm 2$ transition rises continuously when the temperature is lowered from 129 to 4 K, it is concluded that the ground state of **1** is a pair of triplets.

**Acknowledgment.** Support of this research by DGICYT of MEC (Spain) through project PB87-0388 is gratefully acknowledged.

**Registry No. 1**, 135773-36-3; **2**, 14379-95-4; **3**, 135773-37-4; **4**, 135773-38-5; **5**, 135773-39-6; *cis*-dichlorovinylenebis(2,4,6-trichlorobenzene), 135773-40-9; pentachlorobenzene, 608-93-5.

(12) Two diastereoisomers differing only in the propeller helicity of triarylmethyl groups have been recently isolated for the structurally related perchloro-*m*-xylylene.[14]

(13) Wright, B. B.; Platz, M. S. *J. Am. Chem. Soc.* **1983**, *105*, 628.
(14) Veciana, J.; Rovira, C.; Armet, O.; Domingo, V. M.; Crespo, M. I.; Palacio, F. *Mol. Cryst. Liq. Cryst.* **1989**, *176*, 77.

# Surface Raman Scattering of Self-Assembled Monolayers Formed from 1-Alkanethiols: Behavior of Films at Au and Comparison to Films at Ag

**Mark A. Bryant and Jeanne E. Pemberton***

*Contribution from the Department of Chemistry, University of Arizona, Tucson, Arizona 85721.*
*Received March 19, 1991*

**Abstract:** Surface Raman scattering is used to study self-assembled monolayers formed from a series of 1-alkanethiols, $CH_3(CH_2)_nSH$, where $n$ = 3-5, 7, 8, 11, and 17, at mechanically polished and electrochemically roughened Au surfaces. Defect structure in these films is investigated by use of the relative intensities of peaks due to trans and gauche conformations in the $\nu$(C-S) and $\nu$(C-C) frequency regions. Surface selection rules for Raman spectroscopy are used to estimate orientation of the alkanethiol layers at Au. The orientation proposed on the basis of the Raman spectral data is consistent with those previously reported on the basis of other measurements at Au surfaces. This orientation is compared to that previously determined for these films at Ag. Alkanethiols at Ag are found to have a chain tilt from the surface normal less than the 30° previously reported for Au. The C-S bond is found to be perpendicular to the Ag surface while it is largely parallel to the surface at Au. Differences in the spectra of short-chain alkanethiols from smooth and rough surfaces are attributed to disordering of the film at the roughened Au surface which occurs predominantly near the S end of the molecule on rough Au surfaces.

## Introduction

The spontaneous self-assembly of 1-alkanethiols at Au surfaces has been studied with many analytical methods including IR spectroscopy,[1] ellipsometry,[2] XPS,[3] electron diffraction,[4] contact angle measurements,[5] and electrochemistry.[6] In general, the conclusions from these studies are that highly ordered, defect-free monolayer films spontaneously form at Au surfaces.

IR spectroscopy has been commonly used to characterize the packing and orientation of these films.[2,3] IR results suggest that self-assembled monolayer films are densely packed in a crystalline arrangement, with the alkane chain in an all-trans conformation.[3] Comparisons of the frequencies in the $\nu$(C-H) region between adsorbed and solid alkanethiols have been used to deduce con-

* To whom correspondence should be addressed.

(1) Nuzzo, R. G.; Fusco, F. A.; Allara, D. L. *J. Am. Chem. Soc.* **1987**, *109*, 2358.
(2) Porter, M. D.; Bright, T. B.; Allara, D. L.; Chidsey, C. E. D. *J. Am. Chem. Soc.* **1987**, *109*, 3559.
(3) Nuzzo, R. G.; Dubois, L. H.; Allara, D. L. *J. Am. Chem. Soc.* **1990**, *112*, 558.
(4) Strong, L.; Whitesides, G. M. *Langmuir* **1988**, *4*, 546.
(5) Whitesides, G. M.; Laibinis, P. E. *Langmuir* **1990**, *6*, 87.
(6) Finklea, H. O.; Avery, S.; Lynch, M. *Langmuir* **1987**, *3*, 409.

0002-7863/91/1513-8284$02.50/0 

formational information about the C–C bonds.[2,3] Obtaining information directly about the $\nu$(C–C) bands is difficult, because these bands are weak in the IR spectra and are not present in surface spectra.[3] Raman spectroscopy provides valuable information about other important vibrational features of alkanethiols, such as the C–S bond and the carbon backbone, in addition to information in the $\nu$(C–H) region. This report discusses the use of Raman scattering in the $\nu$(C–S), $\nu$(C–C), $\nu$(S–H), and $\nu$(C–H) regions to characterize a series of 1-alkanethiol films at Au. Of particular interest in this work was the utility of Raman scattering for providing direct information on the number and location of gauche conformations in these films.

The tilt angle with respect to the surface normal of long-chain 1-alkanethiols at Au has been calculated from IR spectroscopic data.[2,3] Porter and co-workers propose that the alkane chain is tilted at ca. 20–30° with respect to the surface normal.[2] Nuzzo and co-workers propose the tilt to be ca. 40° with a rotation of 50° about the chain axis.[3] Surface Raman selection rules are used here to qualitatively assess the orientation of the C–S, C–C, and C–H bonds with respect to the Au surface normal. These results are compared to those previously reported for Ag surfaces.[7]

## Experimental Section

**Spectroscopic Conditions and Instrumentation.** Excitation at 514.5 nm was provided by a Coherent Radiation Innova 90-5 $Ar^+$ laser. Excitation at 600 nm was provided by $Ar^+$ laser pumping of a Coherent CR-599 dye laser containing a Rhodamine 6G/ethylene glycol solution. For excitation at 720 nm, a Pyridin 2/propylene carbonate/ethylene glycol solution was used. The laser power incident on the samples was typically 200 mW. The laser beam was focused to a spot of diameter ca. 100 $\mu$m. Spectra of all adsorbed molecules were obtained with light polarized parallel with respect to the plane of incidence. Spectra of bulk alkanethiols were acquired on the neat liquid in a sealed capillary. Solid alkanethiol spectra were acquired by cooling of the capillary with liquid $N_2$ and obtaining spectra with 10-s integrations to prevent laser warming.

Scattered radiation was collected with a Minolta f/1.2 camera lens (50-mm focal length) and focused onto the entrance slit of a Spex 1877 Triplemate. The gratings in the filter stage were 600 grooves/mm, and the grating used in the spectrograph stage was 1200 grooves/mm. Slit widths were typically 0.25 mm/0.3 mm/0.25 mm for 514.5-nm excitation, 0.4 mm/3 mm/0.4 mm for 600-nm excitation, and 0.5 mm/3 mm/0.5 mm for 720-nm excitation. Detection was accomplished with a liquid $N_2$ cooled Photometrics PM512 frontside-illuminated charge-coupled device (CCD). Spectra were acquired at a CCD temperature between −95 and −124 °C. The CCD images were processed with a Photometrics RDS200 system equipped with a custom version of SpectraCalc.

**Electrochemical Conditions and Instrumentation.** The surfaces on which the films were formed were polycrystalline Au disks (Johnson Matthey, 99.999%), which were mechanically polished to a mirror finish with use of 0.05-$\mu$m alumina, rinsed with doubly or triply distilled, deionized water (TDI), and then sonicated for 2 min in TDI water to remove any trapped alumina. A Pt wire served as the auxiliary electrode. Electrode potentials were controlled with an IBM Model EC/225 voltammetric analyzer. Linear potential sweep oxidation–reduction cycles (ORCs) were performed with a simple triangle wave format. Total charge passed during ORCs was monitored with a Princeton Applied Research Model 379 digital coulometer.

**Materials.** 1-Butanethiol (99+%), 1-pentanethiol (98%), 1-hexanethiol (95%), 1-nonanethiol (98%), 1-dodecanethiol (98%), 1-hexadecanethiol (92%), and 1-octadecanethiol (98%) were purchased from Aldrich. Ethanol (absolute) was purchased from Midwest Grain Products. KCl was purchased from Fisher Scientific. Aqueous 1-butanethiolate solutions were made by combining 1 part 1-butanethiol with 9 parts 5 M NaOH. NaOH pellets were purchased from Baker. All were used as received.

**Surface Preparation Procedures.** Spectra were obtained from films at both mechanically polished, mirrored and electrochemically roughened electrodes. To prepare the roughened surfaces, linear potential sweep ORCs were applied to Au electrodes in the presence of 0.1 M aqueous KCl solution. The initial potential was −0.20 V versus a Ag/AgCl reference electrode, and the potential sweep was reversed at ca. +1.20 at a scan rate of 100 mV/s, resulting in ca. 10 mC/cm$^2$ of anodic charge being passed for each cycle. Normally, 20 potential sweeps were used in the roughening procedure for Au.[8] The electrodes were then removed from solution at open-circuit potential, rinsed with 100% ethanol, and finally exposed to the alkanethiol solution. Smooth electrodes were prepared by mechanical polishing as described above before exposure to the alkanethiol solution.

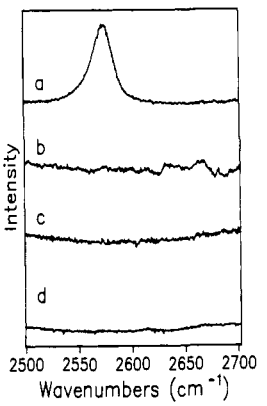


**Figure 1.** Raman spectra in $\nu$(S–H) region (720-nm excitation) of (a) bulk liquid butanethiol, (b) butanethiol adsorbed at smooth Au, (c) butanethiol adsorbed at rough Au, (d) aqueous butanethiolate. Incident power: 150 mW. Integration times: (a) 1 min, (b) 20 min, (c) 1 min, (d) 1 min.

**Film Formation Procedures.** The Au surfaces on which these films were formed are not smooth on an atomic level. Rather, they are envisioned to be gently corrugated with roughness features on the order of the alumina particles used to polish the surface. These surfaces are known to be very weakly enhancing from electromagnetic effects that occur at curved metal surfaces of the appropriate optical properties. The Au surfaces used here are estimated to support an enhancement of ca. 50 at 600-nm excitation relative to a nonenhancing surface.[9] It is highly unlikely that any significant surface roughness of the scale thought to be associated with the "chemical" enhancement mechanism of surface-enhanced Raman scattering (SERS) exists on these surfaces. These distinct sites are known to be very labile and are not likely to survive sonication and transfer steps associated with the surface preparation used here.

For the bands in the $\nu$(C–S) and $\nu$(C–C) region, 720-nm excitation was primarily used to obtain surface spectra of sufficient signal-to-noise ratio. The electromagnetic enhancement of the surface Raman signal for Au is higher at 720 nm than at 600 nm. Excitation at 600 nm was primarily used for the $\nu$(C–H) region where the spectral intensity is greater.

Smooth and roughened surfaces were immersed in alkanethiol solutions in 100% ethanol ranging in concentration from 1 mM for long-chain alkanethiols to 20 mM for short-chain alkanethiols. Samples exposed to 720-nm excitation were immersed in the alkanethiol/ethanol solutions for 2 h to allow the self-assembled monolayers to form. Samples exposed to 600-nm excitation were immersed for ca. 15 h. Surfaces on which films were formed were then rinsed with 100% ethanol and allowed to air dry before spectral data acquisition.

## Results and Discussion

**Formation of Alkanethiol Self-Assembled Monolayer Films.** Formation of 1-alkanethiol monolayers on Au substrates has been proposed to involve cleavage of the S–H bond with concomitant bonding of the S head group to Au.[5] The proposed mechanism shown in Scheme I involves the formation of a Au–S bond, which is thought to be largely covalent with some ionic character.[10]

**Scheme I**

$$RSH + Au_n \underset{-H_2O?}{\overset{-H_2?}{\rightleftharpoons}} RS^-Au^+ + Au_{n-1}$$

Direct evidence for cleavage of the S–H bond is seen in the Raman spectra in the $\nu$(S–H) region shown in Figure 1. The spectrum of neat butanethiol, Figure 1a, shows the very intense $\nu$(S–H) band at ca. 2575 cm$^{-1}$. The S–H band is absent in the surface spectra of butanethiol at both smooth and rough Au

(7) Bryant, M. A.; Pemberton, J. E. *J. Am. Chem. Soc.* **1991**, *113*, 3629.

(8) Corrigan, D. S.; Foley, J. K.; Gao, P.; Pons, S.; Weaver, M. J. *Langmuir* **1985**, *1*, 616.

(9) Sobocinski, R. L.; Bryant, M. A.; Pemberton, J. E. *J. Am. Chem. Soc.* **1990**, *112*, 6177.

(10) Evans, S. D.; Ulman, A. *Chem. Phys. Lett.* **1990**, *170*, 462.

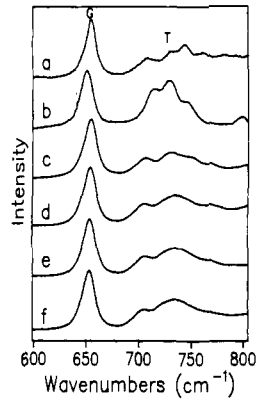


**Figure 2.** Raman spectra in $\nu$(C–S) region (600-nm excitation) of (a) bulk liquid butanethiol, (b) aqueous butanethiolate, (c) bulk liquid pentanethiol, (d) bulk liquid nonanethiol, (e) bulk liquid dodecanethiol, (f) bulk liquid octadecanethiol. Incident power: 250 mW. Integration times: (a) 5 min, (b) 1 min, (c) 1 min, (d) 1 min, (e) 1 min, (f) 1 min.

surfaces, Figure 1, parts a and b, respectively. The disappearance of the $\nu$(S–H) band suggests cleavage of the S–H bond upon adsorption.

Butanethiolate can be formed chemically upon addition of butanethiol to basic aqueous solutions. The spectrum from this species is shown in Figure 1d. The $\nu$(S–H) band is clearly absent in this spectrum, further verifying the thiolate nature of the species adsorbed at Au surfaces. The absence of this band also suggests that no unreacted thiol is present at the Au surface. No $\nu$(S–H) band is observed in surface spectra for any adsorbed alkanethiol studied here. This observation is consistent with the previously reported cleavage of the S–H bond for alkanethiols adsorbed at Ag based on the absence of the $\nu$(S–H) band in spectra from these surfaces.[7,9,11]

The structure of the adsorbed alkanethiol monolayer is dictated by interactions between neighboring alkane chains. With the polar S atom bonded to the Au surface, the nonpolar alkane chains pack in a dense arrangement to maximize van der Waals forces.[12] This arrangement generates densely packed layers which are believed to be crystalline-like.[3]

In the following discussion of the surface Raman spectra for selected alkanethiols ranging from butanethiol to octadecanethiol adsorbed at Au, the surface Raman spectra are compared with Raman spectra of butanethiolate and the corresponding liquid and solid alkanethiols. Comparisons between the solid and liquid spectral behavior are used to assess the crystallinity of the adsorbed layer. Comparisons are also made with alkanethiols adsorbed at roughened Au surfaces which exhibit surface-enhanced Raman scattering. Finally, the results for adsorption at Au are compared with previous results from Ag substrates.[7]

**$\nu$(C–S) Region.** The $\nu$(C–S) region between 600 and 750 cm$^{-1}$ provides conformational information about C–C bonds adjacent to the C–S bond in the alkanethiols. Two $\nu$(C–S) bands are observed in this region as shown in Figure 2a–f for the $n$ = 3, 4, 8, 11, and 17 liquid alkanethiols and butanethiolate. In the liquid alkanethiols, these bands correspond to the gauche (G) $\nu$(C–S) at ca. 655 cm$^{-1}$ and the trans (T) $\nu$(C–S) at 730 cm$^{-1}$. The frequencies of these bands for each molecule are given in Table I. Other bands assigned to T methylene rocks are present in this frequency region at 708 and 762 cm$^{-1}$. The bands at 744 and 782 cm$^{-1}$ are G methylene rocks. These assignments are based on the work of Joo and co-workers who assigned the $\nu(C–S)_G$, $\nu(C–S)_T$, and methylene rocks of butanethiol by comparing the Raman spectra of butanethiolate and butanethiol.[11]

The spectra for the liquid alkanethiols are almost identical in this region. However, the $\nu(C–S)_T$ at ca. 730 cm$^{-1}$ and the methylene rock at ca. 745 cm$^{-1}$ overlap in the longer alkanethiols. The G bands are more intense than the T bands, indicating disorder in the liquid. The $\nu$(C–S) region of butanethiolate is somewhat different from that of butanethiol. While the relative heights of the $\nu(C–S)_G$ and $\nu(C–S)_T$ bands from the thiolate are similar to those observed in the liquid thiol, the G band frequency has shifted down slightly to 650 cm$^{-1}$.

(11) Joo, T. H.; Kim, K.; Kim, M. S. *J. Phys. Chem.* **1986**, *90*, 5816.
(12) Ulman. A.; Eilers, J. G.; Tillman, N. *Langmuir* **1989**, *5*, 1147.

**Table I.** Raman Vibrational Assignments and Peak Frequencies (cm$^{-1}$) in the $\nu$(C–S) Region of $CH_3(CH_2)_nSH$

| | $n$ = 3 | $n$ = 4 | $n$ = 8 | $n$ = 11 | $n$ = 17 | $C_4H_9S^-$ |
|---|---|---|---|---|---|---|
| | | | Liquid | | | |
| $\nu(C–S)_G$ | 655 | 655 | 654 | 654 | 653 | 650 |
| $CH_2$ $rock_T$ | 708 | 707 | 706 | 706 | 706 | 715 |
| $\nu(C–S)_T$ | 731 | 731 | 737 | 737 | 735 | 729 |
| $CH_2$ $rock_G$ | 744 | 750 | | | | 746 |
| $CH_2$ $rock_T$ | 762 | 769 | 770 | 768 | 771 | |
| $CH_2$ $rock_G$ | 782 | | | | | |
| | | | Solid | | | |
| $\nu(C–S)_G$ | 652 | | | | | |
| $CH_2$ $rock_T$ | 706 | 705 | 706 | 706 | 706 | |
| $CH_2$ rock | | 720 | 723 | 726 | | |
| $\nu(C–S)_T$ | 729 | 737 | 732 | 735 | 735 | |
| $CH_2$ $rock_G$ | 741 | | 754 | 749 | 744 | |
| $CH_2$ $rock_T$ | 760 | | | | 759 | |
| | | 802 | 797 | 775 | 780 | |
| | | | | 813 | 806 | |
| | | | Adsorbed at Smooth Au | | | |
| $\nu(C–S)_G$ | 632 | 637 | 641 | 641 | 642 | |
| $\nu(C–S)_T$ | 706 | 706 | 706 | 709 | 713 | |

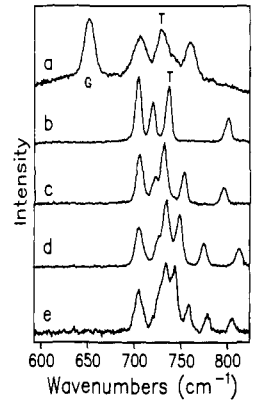


**Figure 3.** Raman spectra in $\nu$(C–S) region (600-nm excitation) of (a) bulk solid butanethiol, (b) bulk solid pentanethiol, (c) bulk solid nonanethiol, (d) bulk solid dodecanethiol, (e) bulk solid octadecanethiol. Incident power: 250 mW. Integration times: (a) 2 min, (b) 0.5 min, (c) 0.5 min, (d) 0.5 min, (e) 0.5 min.

When the neat alkanethiols are cooled to solids with liquid $N_2$, the bands in this region become better resolved and the relative intensities change. Spectra for the $n$ = 3, 4, 8, 11, and 17 solids are shown in Figure 3, parts a–e, respectively. For pentanethiol through octadecanethiol, the $\nu(C–S)_G$ band at ca. 655 cm$^{-1}$ totally disappears from the spectra. This change in relative intensity of the T and G bands is evidence of increased ordering present in the crystalline solid alkanethiols. In butanethiol, there is still significant intensity in the $\nu(C–S)_G$ band and the bands are generally broad, which may be due to incomplete freezing of the material under these conditions.

Upon adsorption of these alkanethiols at smooth Au, the frequencies of both $\nu$(C–S) bands decrease considerably. These spectra are shown in Figure 4, and the frequencies are given in Table I. The $\nu(C–S)_G$ band is observed at ca. 635 cm$^{-1}$ and the $\nu(C–S)_T$ band at ca. 710 cm$^{-1}$. It is more difficult to accurately determine the exact position of the G band because of its low intensity. It is proposed that the frequencies of both $\nu$(C–S) bands are lowered due to the bonding of the S atom to Au. The frequency of the T band shifts to slightly higher frequency as the alkane chain length increases. Thus, the frequency of this band for adsorbed butanethiol is ca. 7 cm$^{-1}$ lower than for adsorbed octadecanethiol.

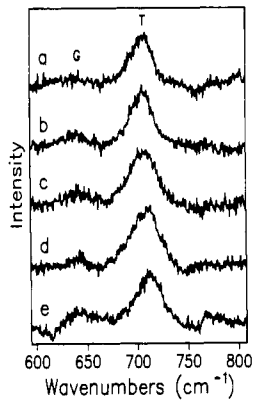


**Figure 4.** Raman spectra in $\nu$(C–S) region (720-nm excitation) of alkanethiols adsorbed at smooth Au: (a) butanethiol, (b) pentanethiol, (c) nonanethiol, (d) dodecanethiol, (e) octadecanethiol. Incident power: 50 mW. Integration times: (a) 5 min, (b) 5 min, (c) 5 min, (d) 5 min, (e) 10 min.

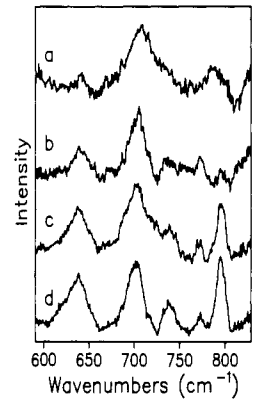


**Figure 5.** Raman spectra in $\nu$(C–S) region (600-nm excitation) of (a) butanethiol adsorbed at smooth Au, (b) butanethiol adsorbed at rough Au (1 ORC), (c) butanethiol adsorbed at rough Au (10 ORCs), (d) butanethiol adsorbed at rough Au (20 ORCs). Incident power: 200 mW. Integration times: (a) 20 min, (b) 5 min, (c) 5 min, (d) 5 min.

A dramatic decrease in $\nu(C-S)_G$ intensity and increase in $\nu(C-S)_T$ intensity are noted upon adsorption of these molecules. This behavior is consistent with an increase in order of these alkanethiols upon adsorption. A similar ratio of T to G intensity is noted for all the alkanethiols studied here, suggesting that the environment around the C–S bond and presumably bonding to the surface are similar for each alkanethiol. The small amount of G intensity may be due to defects in the film at grain boundaries on the polycrystalline Au surface.

A significant difference exists between the surface Raman spectra for alkanethiols adsorbed at smooth Ag[7] and smooth Au. The frequencies of the two $\nu$(C–S) bands are ca. 5–10 $cm^{-1}$ lower on Ag surfaces than on Au surfaces.[7] This disparity suggests that the M–S bond is stronger for Ag than Au and may be the result of greater ionic bonding at Ag than at Au, consistent with the electronegativity differences between S and these two metals. These effects may play an influence in the orientation of the alkanethiol films at Ag and Au as will be discussed below.

The effect of surface roughness on the order of these films is important to assess. A similar ratio of G and T $\nu$(C–S) intensities is noted for dodecanethiol and octadecanethiol at smooth and rough Ag.[7] In contrast, butanethiol exhibits greater G intensity at rough Ag than at smooth Ag.[7] Similarly, smaller chain alkanethiols at rough Au exhibit larger $\nu(C-S)_G$ intensity than at smooth Au, while longer chain alkanethiols show no difference in intensity.

A systematic study of the effect of roughening was performed for butanethiol and octadecanethiol at Au. The spectra from smooth Au surfaces and from Au surfaces subjected to 1, 10, and 20 potential cycle ORCs to produce roughness are shown in Figure 5a–d. The intensity of the $\nu(C-S)_G$ band increases relative to the $\nu(C-S)_T$ band as the number of ORCs increases. In addition, G methylene rocks at ca. 740 and 795 $cm^{-1}$ increase in intensity with the number of ORCs. These effects are not observed for octadecanethiol at Au, suggesting that the roughness features produced in the ORC disorder only short-chain alkanethiol films in the vicinity of the C–S bond.

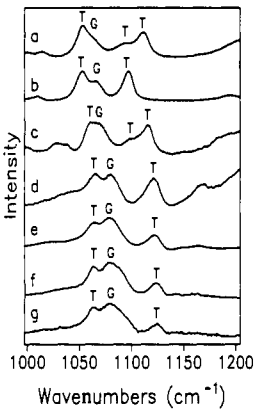


**Figure 6.** Raman spectra in $\nu$(C–C) region (600-nm excitation) of (a) bulk liquid butanethiol, (b) aqueous butanethiolate, (c) bulk liquid pentanethiol, (d) bulk liquid nonanethiol, (e) bulk liquid dodecanethiol, (f) bulk liquid hexadecanethiol, (g) bulk liquid octadecanethiol. Incident power: 200 mW. Integration times: (a) 1 min, (b) 4 min, (c) 4 min, (d) 4 min, (e) 4 min, (f) 1 min, (g) 2 min.

**Table II.** Raman Vibrational Assignments and Peak Frequencies ($cm^{-1}$) in the $\nu$(C–C) Region of $CH_3(CH_2)_nSH$

| | $n = 3$ | $n = 4$ | $n = 8$ | $n = 11$ | $n = 15$ | $n = 17$ | $C_4H_9S^-$ |
|---|---|---|---|---|---|---|---|
| | | | Liquid | | | | |
| | 1014 | | | | | | 1009 |
| | | 1029 | | | | | |
| | | 1038 | | | | | |
| $\nu_a(C-C)_T$ | 1053 | 1061 | 1065 | 1064 | 1063 | 1064 | 1052 |
| $\nu(C-C)_G$ | 1064 | 1070 | 1080 | 1079 | 1079 | 1080 | 1066 |
| $\nu(C-C)_T$ | 1096 | 1099 | | | | | |
| $\nu_s(C-C)_T$ | 1111 | 1116 | 1121 | 1122 | 1123 | 1124 | 1097 |
| | | | Solid | | | | |
| | | | 1051 | 1037 | | | |
| $\nu_a(C-C)_T$ | 1051 | 1058 | 1062 | 1062 | 1062 | 1062 | |
| | | | 1068 | 1084 | 1099 | 1104 | |
| $\nu(C-C)_G$ | | | | | | | |
| $\nu(C-C)_T$ | 1091 | 1101 | 1110 | 1111 | 1110 | 1112 | |
| $\nu_s(C-C)_T$ | 1114 | 1119 | 1127 | 1130 | 1132 | 1130 | |
| | | | 1181 | 1177 | 1175 | 1174 | |
| | | | Adsorbed | | | | |
| | | | Smooth Au | | | | |
| $\nu_a(C-C)_T$ | 1049 | 1054 | 1064 | 1064 | 1064 | 1065 | |
| $\nu(C-C)_G$ | 1063 | | | | | | |
| | | | | 1080 | 1099 | 1103 | |
| $\nu(C-C)_T$ | 1093 | 1103 | | | | | |
| $\nu_s(C-C)_T$ | | | 1120 | 1125 | 1130 | 1129 | |
| | | | Rough Au, Room Temperature | | | | |
| $\nu_a(C-C)_T$ | | | | 1065 | 1065 | | |
| $\nu(C-C)_G$ | | | | | | | |
| | | | | 1082 | 1099 | | |
| $\nu(C-C)_T$ | | | | | | | |
| $\nu_s(C-C)_T$ | | | | 1126 | 1130 | | |
| | | | Rough Au, Subjected to Liquid $N_2$ | | | | |
| $\nu_a(C-C)_T$ | | | | 1064 | 1064 | | |
| $\nu(C-C)_G$ | | | | | | | |
| | | | | 1083 | 1100 | | |
| $\nu(C-C)_T$ | | | | | | | |
| $\nu_s(C-C)_T$ | | | | 1128 | 1132 | | |

**$\nu$(C–C) Region.** The $\nu$(C–C) region contains additional information about the conformational behavior of the alkane chain. *The assignments discussed for this region have been revised from a previous publication*[7] and are discussed in greater detail in a forthcoming publication.[13]

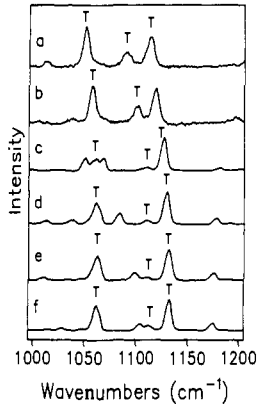


**Figure 7.** Raman spectra in $\nu$(C–C) region (514.5-nm excitation) of (a) bulk solid butanethiol, (b) bulk solid pentanethiol, (c) bulk solid nonanethiol, (d) bulk solid dodecanethiol, (e) bulk solid hexadecanethiol, (f) bulk solid octadecanethiol. Incident power: 150 mW. Integration times: (a) 1 min, (b) 1 min, (c) 1 min, (d) 1 min, (e) 1 min, (f) 1 min.

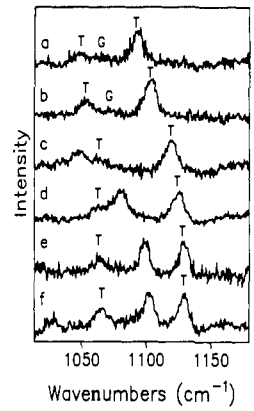


**Figure 8.** Raman spectra in $\nu$(C–C) region (720-nm excitation) of alkanethiols adsorbed at smooth Au: (a) butanethiol, (b) pentanethiol, (c) nonanethiol, (d) dodecanethiol, (e) hexadecanethiol, (f) octadecanethiol. Incident power: 50 mW. Integration times: (a) 5 min, (b) 5 min, (c) 5 min, (d) 5 min, (e) 10 min, (f) 10 min.

The spectra for the liquid alkanethiols in this frequency region are shown in Figure 6, and the peak frequency data are listed in Table II. The band at ca. 1065 $cm^{-1}$ for nonanethiol and longer chains is assigned as the $\nu_a(C–C)_T$, and the band at ca. 1120 $cm^{-1}$ is assigned to the $\nu_s(C–C)_T$.[14] The band at ca. 1080 $cm^{-1}$ is the $\nu(C–C)_G$.[15-19] The frequencies of these bands are slightly lower for pentanethiol and butanethiol. A band at ca. 1100 $cm^{-1}$ has also been assigned to a $\nu(C–C)_T$ in dipalmitoylphosphatidylcholine.[18,19] This $\nu(C–C)_T$ band is seen in liquid butanethiol and pentanethiol at ca. 1100 $cm^{-1}$ and in the spectra of the solid alkanethiols. The G intensity increases with chain length, reflecting the increased possibility of G conformations in longer chains.[20] In contrast to the liquid alkanethiols, the spectrum for butanethiolate shows only three bands in this frequency region.

The spectra for the solid alkanethiols are shown in Figure 7. All three $\nu(C–C)_T$ bands are seen for each of the molecules, but at slightly different frequencies compared to the liquid spectra. For longer chain alkanethiols, the $\nu(C–C)_T$ band at ca. 1120 $cm^{-1}$ shifts to higher frequencies upon solidification, while the $\nu(C–C)_T$ band at ca. 1065 $cm^{-1}$ shifts to slightly lower frequencies. The third $\nu(C–C)_T$ band at ca. 1110 $cm^{-1}$ is seen for all molecules. This band is not seen in the spectra of the long-chain solid alkanes,[21] and its appearance in alkanethiol spectra may be due to the terminal S heteroatom present on the alkane chain. The frequencies of the bands from solid butanethiol and pentanethiol are lower than those of the corresponding alkanethiols of longer chain length.

A fourth band is observed in the spectra for the solid species of nine carbon units and longer. The band appears at ca. 1068 $cm^{-1}$ for nonanethiol, 1084 $cm^{-1}$ for dodecanethiol, 1099 $cm^{-1}$ for hexadecanethiol, and 1104 $cm^{-1}$ for octadecanethiol. Although the band is observed in the spectrum from solid dodecanethiol at the same frequency as the $\nu(C–C)_G$ band appears in the liquid, it is concluded that this band is not the $\nu(C–C)_G$ band. The $\nu(C–C)_G$ bands for liquid nonanethiol, dodecanethiol, hexadecanethiol, and octadecanethiol all are observed at the same frequency of ca. 1080 $cm^{-1}$. In addition, spectra obtained for slightly warmed solid nonanethiol, hexadecanethiol, and octadecanethiol show the fourth band resolved distinctly from the $\nu(C–C)_G$ band. Upon further warming to a liquid, the $\nu(C–C)_G$ band increases in intensity and width and only the $\nu(C–C)_T$ bands at ca. 1065 and 1120 $cm^{-1}$ and the G band are observed.[13] This new band could be one of the many methyl twist or rock vibrations that are observed in this region.[22,23] Additionally, a strong band at 1051 $cm^{-1}$ is observed for solid nonanethiol that is slightly lower in frequency than the $\nu(C–C)_T$ band at 1062 $cm^{-1}$. It is therefore concluded that no intensity from the $\nu(C–C)_G$ is observed for chains of nonanethiol or longer.

The spectra for adsorbed alkanethiols at smooth Au are shown in Figure 8. The spectrum for adsorbed butanethiol in Figure 8a is similar to the spectrum of solution butanethiolate in Figure 6b in that only three bands are observed. This behavior suggests that the adsorbed butanethiol film is more ordered than the bulk liquid. The spectra from adsorbed pentanethiol (Figure 8b) and nonanethiol (Figure 8c) resemble the corresponding solid spectra more than they resemble those of the liquid. Little G intensity is seen for these molecules. For nonanethiol, the band seen at 1051 $cm^{-1}$ in the solid spectrum is also observed in the surface spectrum.

The spectrum of adsorbed dodecanethiol in Figure 8d appears somewhat anomalous in that it is similar to that of the bulk liquid. However, the band at 1078 $cm^{-1}$ is not the $\nu(C–C)_G$ band, but corresponds to the fourth band seen in the solid spectrum at 1084 $cm^{-1}$. Similar behavior was observed in dodecanethiol films at smooth Ag surfaces.[7] Pb underpotential deposition on these films suggests that no gross defects exist.[7] However, there is a small amount of $\nu(C–C)_G$ intensity noted between the 1062-$cm^{-1}$ $\nu(C–C)_T$ band and the band at 1078 $cm^{-1}$. The G component will be discussed in greater detail below.

The spectra for adsorbed hexadecanethiol and octadecanethiol, Figure 8, parts e and f, respectively, are similar to those of the solids. The band at 1098 $cm^{-1}$ for hexadecanethiol and 1100 $cm^{-1}$ for octadecanethiol correspond to the fourth band discussed above. In addition, a small amount of G intensity is noted for the hexadecanethiol film as will be discussed below. In addition, the $\nu(C–C)_T$ band at ca. 1110 $cm^{-1}$ is absent in the surface spectra, suggesting that the films are not as ordered as the bulk solids.

Subtle differences between rough and smooth Au surfaces, and rough Au and Ag surfaces, are noted for the short-chain alkanethiols. The spectra in the $\nu$(C–C) region for butanethiol at rough Au and Ag surfaces are shown in Figure 9, parts a and b, respectively. An increase in the intensity of the 1052-$cm^{-1}$ $\nu_a(C–C)_T$ for butanethiol adsorbed at rough Au, Figure 9a, relative to smooth Au, Figure 8a, is observed. However, the $\nu_a(C–C)_T$ band at 1052 $cm^{-1}$ for rough Ag is less intense than that observed for rough

(13) Joa, S. L.; Bryant, M. A.; Sobocinski, R. L.; Pemberton, J. E. To be published.
(14) Harrand, M. *J. Chem. Phys.* **1983**, *78*, 4777.
(15) Yellin, N.; Levin, I. W. *Biochim. Biophys. Acta* **1977**, *468*, 490.
(16) Gaver, B. P.; Peticolas, W. L. *Biochim. Biophys. Acta* **1977**, *465*, 260.
(17) Spiker, R. C.; Levin, I. W. *Biochim. Biophys. Acta* **1976**, *433*, 457.
(18) Yellin, N.; Levin, I. W. *Biochemistry* **1977**, *16*, 642.
(19) Gaber, B. P.; Yager, P.; Peticolas, W. L. *Biophys. J.* **1978**, *21*, 161.
(20) Maissara, M.; Devaure, J. *J. Raman. Spec.* **1987**, *18*, 181.
(21) Royaud, I. A. M.; Hendra, P. J.; Maddams, W.; Passingham, C.; Willis, H. A. *J. Mol. Struct.* **1990**, *239*, 83.
(22) Snyder, R. G.; Schachtshneider, J. H. *Spectrochim. Acta* **1963**, *19*, 85.
(23) Schachtshneider, J. H.; Snyder, R. G. *Spectrochim. Acta* **1963**, *19*, 117.
(24) Snyder, R. G.; Cameron, D. G.; Casal, H. L.; Compton, D. A. C.; Mantsch, H. H. *Biochim. Biophys. Acta* **1982**, *684*, 111.

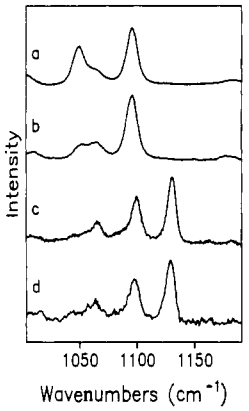


**Figure 9.** Raman spectra in $\nu$(C–C) region of butanethiol adsorbed at (a) rough Au (20 ORCs) and (b) rough Ag and hexadecanethiol adsorbed at (c) rough Au (20 ORCs) and (d) rough Ag. Excitation: (a) 720 nm, (b) 600 nm, (c) 720 nm, (d) 514.5 nm. Incident power: 50 mW (720-nm excitation), 200 mW (514.5- and 600-nm excitation). Integration times: (a) 5 min, (b) 1 min, (c) 10 min, (d) 1 min.

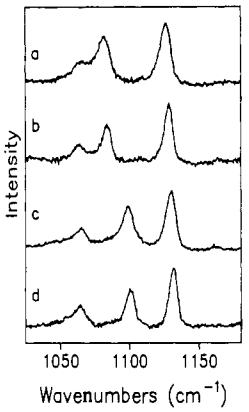


**Figure 10.** Raman spectra in $\nu$(C–C) region (720-nm excitation): of dodecanethiol adsorbed at rough Au (20 ORCS) (a) room temperature, (b) subjected to liquid $N_2$; of hexadecanethiol adsorbed at rough Au (20 ORCs) (c) room temperature, (d) subjected to liquid $N_2$. Incident power: 50 mW. Integration times: (a) 1 min, (b) 1 min, (c) 1 min, (d) 1 min.

Au. This difference is proposed to be due to the slightly different tilt angles of the molecules at Ag and Au and will be discussed in the section on Orientation of Alkanethiols at Au and Ag. Hexadecanethiol at rough Au and rough Ag are shown in Figure 9, parts c and d, respectively. The spectrum at rough Au, Figure 9c, exhibits a slightly different intensity of the 1098 $cm^{-1}$ band relative to that observed at smooth Au, Figure 8e. The spectra obtained at rough Au and rough Ag are very similar for this molecule. Thus, roughening is concluded to strongly influence the conformations of the bonds near the surface as in butanethiol, for example, but not further out along the alkane chains in the molecules. Similar behavior is observed on smooth and rough Ag surfaces.[7]

The relative G components of films of dodecanethiol and hexadecanethiol were further investigated. The films were subjected to liquid $N_2$ cooling, and the changes in the $\nu$(C–C) region were observed. Parts a and b of Figure 10 show the spectra for dodecanethiol at rough Au at room temperature and after exposure to liquid $N_2$, respectively. The spectra for hexadecanethiol at rough Au at room temperature and after exposure to liquid $N_2$ are shown in Figure 10, parts c and d, respectively. The spectra for films of both molecules subjected to liquid $N_2$ cooling exhibit a decrease in G intensity in the region between the $\nu_a(C–C)_T$ and the fourth band. Additionally, the T bands are narrower and closer in frequency to the solid alkanethiol spectra. The frequencies are listed in Table II.

The spectra were subjected to curve-fitting procedures to estimate the G component in these films. For hexadecanethiol at rough Au exposed to liquid $N_2$, the intensity of the 1080-$cm^{-1}$ $\nu(C–C)_G$ band is estimated to be less than 1% of the intensity of the 1130-$cm^{-1}$ $\nu(C–C)_T$ band. The room temperature spectrum was fit as follows. First, the spectrum for hexadecanethiol film exposed to liquid $N_2$ was subtracted from the spectrum obtained at room temperature. Then, the difference spectrum was curve fit for G band intensity. From this fitting, the G band intensity in the room temperature films is estimated to be ca. 20% of the intensity of the 1130-$cm^{-1}$ $\nu(C–C)_T$ band. For dodecanethiol at room temperature, the relative G band intensity is estimated by this procedure to be ca. 25%. The numbers should not be taken as absolute indicators of the amount of defect structure in these films. The absolute degree of disordering in the surface films may actually be smaller than estimated, because the changes in $\nu(C–C)_G$ and $\nu_s(C–C)_T$ intensities may not be linear with the number of G conformers in the chain.[24]

**Table III.** Raman Vibrational Assignments and Peak Frequencies ($cm^{-1}$) in the $\nu$(C–H) Region of $CH_3(CH_2)_nSH$

| | $n = 3$ | $n = 4$ | $n = 8$ | $n = 11$ | $n = 17$ | $C_4H_9S^-$ |
|---|---|---|---|---|---|---|
| | | | Liquid | | | |
| $\nu_s(CH_2)$ | 2848 | | 2850 | 2850 | 2850 | 2845 |
| $\nu_s(CH_2)$ | 2864 | 2858 | | | | 2863 |
| $\nu_s(CH_3)$ | 2875 | 2873 | 2873 | 2873 | 2873 | 2876 |
| $\nu_a(CH_2)$ | 2905 | 2895 | 2896 | 2896 | 2892 | 2903 |
| $\nu_s(CH_2,FR)$ | 2914 | 2914 | | | | 2914 |
| $\nu_s(CH_2,FR)$ | 2926 | 2926 | 2926 | 2927 | 2927 | |
| $\nu_s(CH_3,FR)$ | 2936 | 2935 | | | | 2938 |
| $\nu_a(CH_3)$ | 2964 | 2960 | 2958 | 2959 | 2961 | 2964 |
| | | | Solid | | | |
| $\nu_s(CH_2)$ | 2842 | | | 2849 | 2849 | |
| $\nu_s(CH_2)$ | 2857 | 2854 | 2858 | 2859 | 2858 | |
| $\nu_s(CH_3)$ | 2873 | 2872 | 2869 | 2871 | 2871 | |
| $\nu_a(CH_2)$ | | | 2882 | 2883 | 2883 | |
| $\nu_a(CH_2)$ | 2900 | 2892 | 2895 | 2898 | 2904 | |
| $\nu_s(CH_2,FR)$ | | | 2915 | 2913 | | |
| $\nu_s(CH_2,FR)$ | 2925 | 2924 | 2926 | 2924 | 2924 | |
| $\nu_s(CH_3,FR)$ | 2937 | | | | | |
| $\nu_a(CH_3)_{oop}$ | 2956 | 2953 | 2952 | | | |
| $\nu_a(CH_3)_{ip}$ | 2968 | 2968 | 2966 | 2958 | 2957 | |
| | | | Adsorbed at Smooth Au | | | |
| $\nu_s(CH_2)$ | | | 2854 | 2853 | 2851 | |
| $\nu_s(CH_2)$ | 2854 | 2852 | | | | |
| $\nu_s(CH_3)$ | 2875 | 2876 | | | | |
| $\nu_a(CH_2)$ | | | 2880 | 2879 | 2883 | |
| $\nu_a(CH_2)$ | | | 2907 | 2904 | 2903 | |
| $\nu_s(CH_2,FR)$ | 2908 | 2909 | | 2916 | | |
| $\nu_s(CH_2,FR)$ | | | | | | |
| $\nu_s(CH_3,FR)$ | 2936 | 2938 | 2936 | 2932 | 2932 | |
| $\nu_a(CH_3)$ | 2964 | 2966 | 2967 | 2963 | 2965 | |

**$\nu$(C–H) Region.** The $\nu$(C–H) region is quite complex and contains at least 10 bands.[23,25] These bands include $\nu_{sym}$ and $\nu_{asym}$ modes of methyl and methylene groups and Fermi resonances of the vibrations with $\delta$(C–H) overtones. The spectra for liquid alkanethiols and butanethiolate are shown in Figure 11, and the bands and their assignments are tabulated in Table III. Two $\nu_{sym}(CH_2)$ bands are seen at ca. 2850 and 2860 $cm^{-1}$. The 2860-$cm^{-1}$ band corresponds to the $\nu_{sym}(CH_2)$ adjacent to the methyl group, while the other band corresponds to the remaining methylene groups. The lower frequency band is more intense in the long-chain alkanethiols. Two bands due to the Fermi resonance of the $\nu_{sym}(CH_2)$ band with the overtone of the $\delta(CH_2)$ band appear at ca. 2913 and ca. 2927 $cm^{-1}$. The $\nu_{sym}(CH_2,FR)$ band at 2913 $cm^{-1}$ is a shoulder on the broad $\nu_{asym}(CH_2)$ band for dodecanethiol and octadecanethiol. The $\nu_{asym}(CH_2)$ band appears at ca. 2905 $cm^{-1}$ for butanethiol and shifts to lower frequencies as the chain length increases, reaching 2892 $cm^{-1}$ in octadecanethiol.

The $\nu_{sym}(CH_3)$ band appears at ca. 2873 $cm^{-1}$, and the $\nu_{sym}(CH_3,FR)$ band is observed 2935 $cm^{-1}$. The $\nu_{asym}(CH_3)$ band appears at ca. 2960 $cm^{-1}$ in these spectra. Both the $\nu_{sym}(CH_3)$

(25) Snyder, R. G.; Strauss, H. L.; Elliger, C. A. *J. Phys. Chem.* **1982**, *86*, 5145.

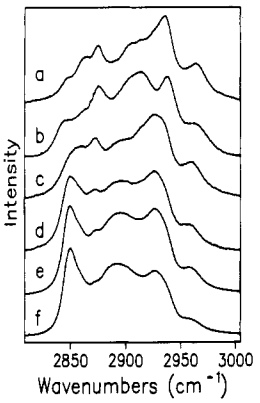


**Figure 11.** Raman spectra in $\nu$(C–H) region (600-nm excitation) of (a) bulk liquid butanethiol, (b) aqueous butanethiolate, (c) bulk liquid pentanethiol, (d) bulk liquid nonanethiol, (e) bulk liquid dodecanethiol, (f) bulk liquid octadecanethiol. Incident power: 100 mW. Integration times: (a) 1 min, (b) 1 min, (c) 5 min, (d) 5 min, (e) 1 min, (f) 1 min.

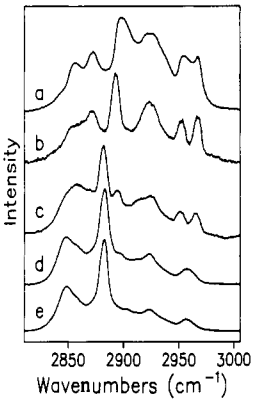


**Figure 12.** Raman spectra in $\nu$(C–H) region (600-nm excitation) of (a) bulk solid butanethiol, (b) bulk solid pentanethiol, (c) bulk solid nonanethiol, (d) bulk solid dodecanethiol, (e) bulk solid octadecanethiol. Incident power: 100 mW. Integration times: (a) 3 min, (b) 2 min, (c) 2 min, (d) 2 min, (e) 2 min.

and $\nu_{asym}(CH_3)$ bands decrease in intensity relative to the methylene bands as the chain length increases, reflecting the increase in number of methylene groups.

These bands are more resolved in the spectra of the solid alkanethiols as shown in Figure 12. The assignments are similar to those in the liquids; however, some notable changes are observed. The $\nu_{asym}(CH_3)$ band is split into two bands at 2952 and 2966 cm$^{-1}$ for butanethiol, pentanethiol, and nonanethiol. The lower frequency band has been assigned to the out-of-plane $\nu_{asym}(CH_3)$ and the higher frequency band to the in-plane $\nu_{asym}(CH_3)$.[26] The $\nu_{sym}(CH_3)$ and $\nu_{sym}(CH_3,FR)$ bands at ca. 2870 and ca. 2935 cm$^{-1}$ are weak in intensity for nonanethiol through octadecanethiol. The strong band at 2883 cm$^{-1}$ is assigned to the $\nu_{asym}(CH_2)$. In fact, the $\nu_{asym}(CH_2)$ is split into a strong band at 2883 cm$^{-1}$ and a weaker band at ca. 2900 cm$^{-1}$ for nonanethiol, dodecanethiol, and octadecanethiol.

The spectra for the adsorbed alkanethiols are shown in Figure 13. From the spectrum in Figure 13a, it can be seen that adsorbed butanethiol resembles more closely the spectrum of butanethiolate, Figure 11b, than that of liquid or solid butanethiol. Both adsorbed butanethiol and aqueous butanethiolate exhibit a large decrease in the intensity of the $\nu_{sym}(CH_2,FR)$ at 2925 cm$^{-1}$. The relative intensity of the $\nu(CH_3)$ to $\nu(CH_2)$ bands is larger for adsorbed butanethiol than for aqueous butanethiolate. The other adsorbed alkanethiols also show a large increase in the relative intensity of the $\nu(CH_3)$ bands to $\nu(CH_2)$ bands as compared to those in the liquid spectra.

(26) MacPhail, R. A.; Snyder, R. G.; Strauss, H. L. *J. Chem. Phys.* **1982**, *77*, 1118.

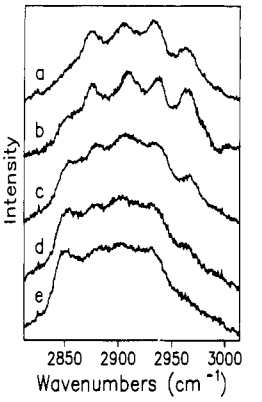


**Figure 13.** Raman spectra in $\nu$(C–H) region (600-nm excitation) of alkanethiols adsorbed at smooth Au: (a) butanethiol, (b) pentanethiol, (c) nonanethiol, (d) dodecanethiol, (e) octadecanethiol. Incident power: 100 mW. Integration times: (a) 20 min, (b) 5 min, (c) 20 min, (d) 20 min, (e) 20 min.

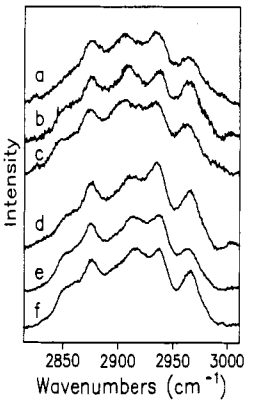


**Figure 14.** Raman spectra in $\nu$(C–H) region (600-nm excitation): of alkanethiols at smooth Au: (a) butanethiol, (b) pentanethiol, (c) hexanethiol; of alkanethiols adsorbed at smooth Ag (d) butanethiol, (e) pentanethiol, (f) hexanethiol. Incident power: 100 mW. Integration times: (a) 20 min, (b) 5 min, (c) 20 min, (d) 5 min, (e) 5 min, (f) 5 min.

The relative intensity of the $\nu_{asym}(CH_3)$ band to the $\nu_{sym}(CH_3)$ band also contains significant information. Even though the $\nu_{asym}(CH_3)$ intensity in the bulk liquid spectra generally decreases with increasing chain length, the relative intensity of the $\nu_{asym}(CH_3)$ for adsorbed pentanethiol is stronger than that for adsorbed butanethiol. The spectra for adsorbed butanethiol, pentanethiol, and hexanethiol at smooth Au shown in Figure 14, parts a–c, respectively, illustrate the significance of the relative intensity behavior of the $\nu(CH_3)$ bands. These spectra have been plotted so that the $\nu_{sym}(CH_3)$ bands of each adsorbed alkanethiol spectrum are of the same intensity. On this intensity scale, a greater $\nu_{asym}(CH_3)$ intensity is observed for the odd-numbered pentanethiol than for the even-numbered butanethiol and hexanethiol. In contrast, alkanethiols adsorbed to Ag show the opposite behavior, as shown in Figure 14d–f. The spectra at Ag are similar in all respects to those at Au, except that the intensity of the $\nu_{asym}(CH_3)$ band is greater for the even-numbered chains (butanethiol and hexanethiol) than for the odd-numbered chains. Although not shown, similar behavior is observed for the relative $\nu(CH_3)$ intensities for octanethiol and nonanethiol at Au and Ag. The orientation of the terminal methyl group, and hence that of the carbon backbone with respect to the surface normal, can be deduced from this behavior. The details of this analysis and models for adsorption and orientation of these molecules at Au and Ag based on these data are presented below.

Spectra from rough Au surfaces differ slightly from those at smooth surfaces as demonstrated by the spectra in Figure 15. The spectra in Figure 15a–c are from butanethiol, pentanethiol, and hexanethiol, respectively, adsorbed at Au roughened with 20 ORCs. The $\nu(CH_3)$ bands are slightly stronger in the surface spectra from the rough Au. The odd–even effect is still clearly

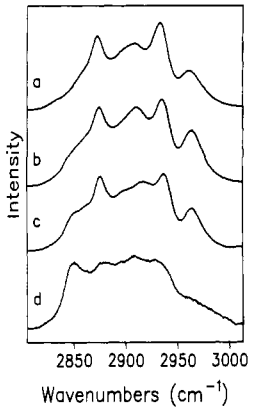


**Figure 15.** Raman spectra in $\nu$(C–H) region (600-nm excitation) of (a) butanethiol adsorbed at rough Au (20 ORCs), (b) pentanethiol adsorbed at rough Au (20 ORCs), (c) hexanethiol adsorbed at rough Au (20 ORCs), (d) octadecanethiol adsorbed at rough Au (20 ORCs). Incident power: 200 mW. Integration times: (a) 1 min, (b) 1 min, (c) 5 min, (d) 5 min.

evident for the $\nu_{asym}(CH_3)$ band. The spectrum for octadecanethiol at rough Au, shown in Figure 15d, differs from spectra at smooth Au to a lesser degree. Similar behavior is observed for alkanethiols at rough and smooth Ag.[7] This observation is consistent with the behavior in the $\nu$(C–C) region as discussed above. Thus, the roughening procedure appears to introduce disorder in the film adjacent to the Au surface, but the disorder is not significantly increased in the rest of the alkane chain.

**Orientation of Alkanethiols at Au and Ag.** The orientation of alkanethiols at Au substrates has been investigated by several groups. Ulman and co-workers have used computer modeling to calculate the free energies of various orientations of long-chain alkanethiols.[12] The tilt and rotation angles of adsorbed alkanethiols were predicted from the minima in free energy of the systems based on van der Waals interactions between adjacent molecules at single crystals of Au. The lowest free energy was found for a molecular tilt of the carbon backbone of ca. 30° from normal with a rotation about the chain axis of ca. 55°. Bareman and Klein have also calculated molecular tilt as a function of area per chain using molecular dynamics simulations. An average tilt of ca. 30° was calculated for a nearest-neighbor spacing of 5.0 Å.[27] This spacing corresponds to the spacing of next-nearest atoms for the Au(111) surface.[4]

Nuzzo and co-workers have estimated a tilt angle of ca. 40° from the surface normal for long-chain alkanethiols at Au with a rotation about the chain axis of 50° from IR spectral data interpreted on the basis of surface selection rules.[3] Porter and co-workers proposed the chain tilt to be ca. 20–30° using IR spectroscopy and ellipsometry.[2] Using electron diffraction, Strong and Whitesides estimated the tilt angle to be 25–35°.[4]

Orientation of alkanethiols at Au and Ag can also be qualitatively deduced from Raman spectroscopy with use of surface selection rules. In addition to orientation of the methyl and methylene groups, the orientation of the C–S bond and carbon backbone can be inferred. These rules are often called "propensity rules",[28] because the magnitude of the dielectric constants in the visible wavelength region results in less rigorous rules than those operative in the infrared. These rules have been elegantly described by Moskovits[29] and Creighton[30] for rough surfaces. Recently, Gao and co-workers have demonstrated the utility of these rules for the determination of orientation of benzene and benzene analogues at rough Au.[31]

The fundamental basis of these rules according to the Moskovits treatment is as follows.[29] Consider a surface in which the coordinate frame is defined such that the $z$ axis is perpendicular to the surface and the $x$ and $y$ axes are parallel to the surface. With excitation to the red of the surface plasmon wavelength, vibrations of surface-confined molecules with a component along the $z$ axis will be enhanced more than vibrations without a $z$ component. More specifically, vibrations with $zz$ tensor components will be enhanced to a larger extent than vibrations with $xz$ or $yz$ components. Vibrations of the molecule having large components along the $x$ or $y$ axes will be only weakly enhanced.

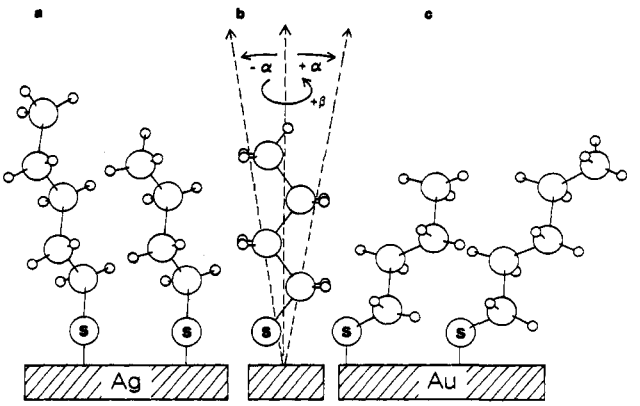


**Figure 16.** Models of orientation of 1-alkanethiols at Ag and Au surfaces: (a) adsorption at Ag, chain tilt ($\alpha$) of ca. −15° and rotation ($\beta$) of ca. 45° about chain axis; (b) adsorption at surface with $\alpha$ and $\beta$ of 0°; (c) adsorption at Au, $\alpha$ of ca. +30° and $\beta$ of ca. 45°.

1-Alkanethiol molecules have very low symmetry and belong, at best, in the $C_s$ point group. In this point group, all vibrations of the adsorbed molecule have a component perpendicular to the surface in all orientations. The relative contributions of the various tensor components to the polarizability of a vibration are generally not known.[30] Stretching vibrations, however, are assumed to have a larger contribution from the tensor component along the axis of the vibration. Gao and co-workers have concluded this to be true of the $\nu$(C–H) vibration in benzene and toluene from their SERS spectra at Au surfaces.[31] Stretching vibrations can therefore be used for interpretation of orientation in these alkanethiol systems. Stretches that are orthogonal will be enhanced by different amounts when the Raman surface spectra are compared to those of the bulk liquid molecules.[32] For the treatment presented here, the methylene stretches are assumed to be largely orthogonal to the C–C and C–S stretches and the $\nu_{asym}(CH_3)$ are assumed to be largely orthogonal to the $\nu_{sym}(CH_3)$ vibrations. Harrand has concluded that the $\nu_a(C-C)_T$ band has $xz$ polarizability and the $\nu_s(C-C)_T$ has $zz$ polarizability in dipalmitoylphosphatidylcholine.[14] In this work, the axes have been defined such that the $z$ axis is parallel to the alkane chain and the $x$ axis is perpendicular to the plane of the carbon backbone of the carbon chain.

Figure 16 shows models of butanethiol and pentanethiol at Au and Ag substrates. Figure 16b shows butanethiol with the chain axis perpendicular to the surface. Figure 16c shows models of butanethiol and pentanethiol adsorbed at Au previously proposed with a carbon backbone tilt of ca. 30° with a rotation about the chain axis of ca. 45°. In this orientation, the C–S bonds are largely parallel to the surface. For butanethiol in this orientation, the $\nu_{sym}(CH_3)$ dipole is largely perpendicular to the surface along the direction of the $C_3$–$C_4$ bond. For pentanethiol in this orientation, the $\nu_{sym}(CH_3)$ dipole is largely parallel to the surface along the direction of the C–S bond.

This picture of alkanethiol orientation at Au is consistent with that proposed from IR data by Nuzzo and co-workers. In their previous study, the $\nu_{sym}(CH_3)$ and $\nu_{asym}(CH_3)$ intensities for heptadecanethiol and octadecanethiol adsorbed at Au were compared.[3] While the intensities of the two methyl stretches were found to be similar for octadecanethiol, the $\nu_{asym}(CH_3)$ was noted

(27) Bareman, J. P.; Klein, M. L. *J. Phys. Chem.* **1990**, *94*, 5202.
(28) Otto, A. *Colloids Surf.* **1989**, *38*, 27.
(29) Moskovits, M. *Rev. Mod. Phys.* **1985**, *57*, 783.
(30) Creighton, J. A. In *Spectroscopy of Surfaces*; Clark, R. J. H., Hester, R. E., Eds.; John Wiley: New York, 1988; p 37.
(31) Gao, X.; Davies, J. P.; Weaver, M. J. *J. Phys. Chem.* **1990**, *94*, 6858.
(32) Pemberton, J. E.; Bryant, M. A.; Sobocinski, R. L.; Joa, S. L. *J. Phys. Chem.*, in press.

Table IV. Peak Area Ratios for $\nu$(C-S), $\nu$(C-C), and $\nu$(C-H) Regions in Bulk and Adsorbed Alkanethiols

| | $(I_{(C-S)_{ads}}/I_{(C-H)_{ads}})/(I_{(C-S)_{bulk}}/I_{(C-H)_{bulk}})$ | | $(I_{(C-C)_{ads}}/I_{(C-H)_{ads}})/(I_{(C-C)_{bulk}}/I_{(C-H)_{bulk}})$ | |
|---|---|---|---|---|
| | Ag | Au | Ag | Au |
| butanethiol | 3.2 | 0.7 | 3.9 | 1.6 |
| pentanethiol | 6.8 | 0.6 | 5.7 | 2.1 |

to be more intense than the $\nu_{sym}(CH_3)$ for heptadecanethiol. Thus, the model proposed for the odd-numbered chain pentanethiol in Figure 16c is similar to that proposed by Nuzzo for orientation of heptadecanethiol, and that for butanethiol is similar to Nuzzo's for octadecanethiol.

A similar analysis of the remainder of the surface Raman data was undertaken for butanethiol and pentanethiol at smooth Au and compared to that from smooth Ag surfaces. The ratio of the intensity of the combined $\nu$(C-S) bands to the entire $\nu$(C-H) region in the surface spectra was calculated and divided by the ratio of the $\nu$(C-S) to $\nu$(C-H) bands in the bulk liquid spectra. The resulting values are reported in Table IV. Also reported are the $\nu$(C-C)/$\nu$(C-H) surface ratios divided by the $\nu$(C-C)/$\nu$(C-H) bulk liquid ratios. For both butanethiol and pentanethiol at Au, the $\nu$(C-S)/$\nu$(C-H) surface/liquid ratio is less than 1. This result agrees with the model proposed in Figure 16c, because the decrease in surface $\nu$(C-S) intensity strongly implies that the C-S bond is largely parallel to the surface. On the other hand, the $\nu$(C-C)/$\nu$(C-H) surface/liquid ratio for the adsorbed molecule at Au is greater than 1, which suggests that the carbon backbone is more perpendicular to the surface than the C-S bond. This picture is also consistent with the model shown in Figure 16c.

The model further predicts that the methyl group is largely perpendicular to the surface for butanethiol and largely parallel to the surface for pentanethiol. This change in methyl group orientation with chain length is supported by the relative intensities of the $\nu(CH_3)$ bands of the surface Raman spectra shown in Figure 14 and discussed above. The $\nu_{sym}(CH_3)$ is a totally symmetric band while the $\nu_{asym}(CH_3)$ is expected to have polarizability tensors greatest in the direction orthogonal to the carbon backbone. Hence, the ratio of the $\nu_{asym}(CH_3)$ intensity to the $\nu_{sym}(CH_3)$ intensity can be used to deduce the orientation of the methyl group of the adsorbed alkanethiol.[32] As shown in Figure 14, the $\nu_{asym}(CH_3)$ band is stronger for pentanethiol at Au and weaker for butanethiol and hexanethiol at Au relative to the $\nu_{sym}(CH_3)$ band. Thus, based on surface selection rules, the $\nu_{asym}(CH_3)$ vibration for pentanethiol at Au is largely perpendicular to the surface. The $C_4$-$C_5$ bond, and hence the methyl dipole, is directed largely parallel to the surface, because the $\nu_{asym}(CH_3)$ polarizability tensor is presumed to be orthogonal to the $C_4$-$C_5$ bond. Based on similar arguments, the methyl dipole must be largely perpendicular to the surface for butanethiol.

As demonstrated by the data in Table IV, the intensity ratio behavior for alkanethiols adsorbed at Ag is significantly different from that measured from Au substrates. The $\nu$(C-S)/$\nu$(C-H) surface/liquid ratio for butanethiol and pentanethiol is greater than 1 for Ag, suggesting that the C-S bond is largely perpendicular to the Ag surface. In addition, the $\nu$(C-C)/$\nu$(C-H) surface/liquid ratio is also greater than 1 for these alkanethiols. The enhancement of the surface $\nu$(C-C) bands at Ag is greater than at Au, which suggests that the tilt angle of the alkanethiols at Ag is less than that at Au. Based on IR spectroscopy, Ulman and co-workers have proposed that the chain tilt angle of octadecanethiol at Ag is less than that at Au.[33]

In addition, it is observed that the $\nu_a(C-C)_T$ band at 1052 $cm^{-1}$ is larger in intensity than the 1093-$cm^{-1}$ $\nu(C-C)_T$ and the 1063-$cm^{-1}$ $\nu(C-C)_G$ bands for butanethiol at rough Au relative to rough Ag, as shown in Figure 9, parts a and b, respectively. The polarizability of the $\nu_s(C-C)_T$ band is largely along the alkane chain while the $\nu_a(C-C)_T$ has polarizability components along and perpendicular to the alkane chain.[14] However, the polarizabilities of the $\nu$(C-C) bands at 1093 and 1065 $cm^{-1}$ have not been determined. The relative intensity of the $\nu_a(C-C)_T$ band is predicted and observed to be larger for an alkane chain that is more parallel to the surface as is the case for Au as compared to Ag. These results additionally suggest that the polarization of the $\nu(C-C)_T$ at 1093 $cm^{-1}$ is similar to that of $\nu_s(C-C)_T$.

Consistent with the difference in C-S bond behavior at Ag and Au, the methyl group orientation at Ag is also different from that at Au for these molecules. The ratio of $\nu_{asym}(CH_3)$ to $\nu_{sym}(CH_3)$ intensity is greater for butanethiol than for pentanethiol at Ag. This behavior is opposite to that observed at Au. It is therefore deduced that the $C_3$-$C_4$ bond, and hence the methyl dipole, is more parallel to the surface for butanethiol but is more perpendicular for pentanethiol at Ag.

Figure 16a shows models for butanethiol and pentanethiol adsorbed at Ag. The chain tilt angle is ca. −15°, opposite in direction to that shown for alkanethiols at Au in Figure 16c, and the rotation about the chain axis is ca. 45°. A similar orientation can be achieved with a tilt of ca. +15° and a rotation of ca. 135°.

Walczak and co-workers have recently presented results from a study of alkanethiol monolayers at Ag and Au using IR spectroscopy.[34] The tilt angle was calculated to be ca. −13°, opposite in direction to that observed at Au, with a rotation about the chain axis of ca. 45°. The odd–even behavior of the two $\nu(CH_3)$ bands was observed at Ag for short-chain alkanethiols up to nonanethiol. It was suggested that the metal-S bonding strongly influenced the different orientations at Au and Ag.

The surface Raman spectra in the $\nu$(C-S) support the argument of significant differences in metal-S bonding at the two substrates. The $\nu(C-S)_T$ frequencies are ca. 4 $cm^{-1}$ lower for alkanethiols on Ag than on Au. The models shown in Figure 15 suggest more $\pi$ interaction of the S lone pairs with Ag than with Au. Studies concerning the potential dependence of the orientation of these molecules in electrochemical environments have provided important insight into the effect of surface electronegativities upon the metal-S bonding. These results will be reported shortly.[35]

## Conclusions

Surface Raman scattering has been used to characterize self-assembled monolayers formed from alkanethiols at mechanically polished, mirrored, and electrochemically roughened Au surfaces. Raman scattering is an extremely useful technique for investigating self-assembling alkanethiol monolayers, because vibrational information can be obtained from all locations within the molecule. For example, insight into ordering of the monolayer and defects within the alkane chains can be directly investigated by measuring the intensity of the G band associated with the carbon backbone. From these bands, it is concluded that the alkane chain of adsorbed alkanethiols is mostly in the all-T conformation, and the amount of G conformers has been estimated for films formed from long-chain alkanethiols. The conformations adjacent to the C-S bond are mostly T for all alkanethiols, although a small amount of G is consistently detected.

Surface selection rules are used to develop a clear picture of the orientation of these molecules at Au and Ag. Different metal-S bonding interactions result in different C-S bond orientations at Ag and Au. The C-S bond is largely parallel to the surface at Au and mostly perpendicular at Ag. This difference in bonding between the two metals in turn affects the chain tilt angle and rotation of the alkanethiols. Alkanethiols at Ag orient with a smaller chain tilt angle from the surface normal than at Au. The results presented here agree with previous determinations of orientation on these two metals.

The Raman scattering obtained from rough Au surfaces exhibits more G conformations around the C-S bond adjacent to the surface than observed at smooth surfaces. The difference was more pronounced than that found for rough and smooth Ag, probably due to the different roughening procedures employed.

(33) Ulman, A. *J. Mater. Educ.* **1989**, *11*, 205.

(34) Walczak, M. M.; Chung, C.; Stole, S. M.; Widrig, C. A.; Porter, M. D. *J. Am. Chem. Soc.* **1991**, *113*, 2370.

(35) Bryant, M. A.; Pemberton, J. E. *J. Am. Chem. Soc.*, submitted for publication.

Similar spectra were obtained in the $\nu$(C–C) and $\nu$(C–H) regions for all surfaces, suggesting that disordering induced by surface roughness is most easily accommodated by disruption of van der Waals bonding near the S end of the molecule.

**Acknowledgment.** We are grateful for support of this work by the National Science Foundation (CHE-8614955). Helpful discussions with Dr. Marc D. Porter are also gratefully acknowledged.

**Registry No.** Au, 7440-57-5; $CH_3(CH_2)_3SH$, 109-79-5; $CH_3(CH_2)_4SH$, 110-66-7; $CH_3(CH_2)_5SH$, 111-31-9; $CH_3(CH_2)_7SH$, 94805-33-1; $CH_3(CH_2)_8SH$, 1455-21-6; $CH_3(CH_2)_{11}SH$, 1322-36-7; $CH_3(CH_2)_{17}SH$, 2885-00-9.

# An ab Initio Study (6-31G*) of Transition States in Glycoside Hydrolysis Based on Axial and Equatorial 2-Methoxytetrahydropyrans[1]

**C. Webster Andrews,[†,2a] Bert Fraser-Reid,*[,†] and J. Phillip Bowen[‡,2b]**

*Contribution from the Paul M. Gross Chemical Laboratory, Department of Chemistry, Duke University, Durham, North Carolina 27706, and Laboratory for Molecular Modeling, Division of Medicinal Chemistry and Natural Products, School of Pharmacy, University of North Carolina at Chapel Hill, Chapel Hill, North Carolina 27599.* *Received May 6, 1991*

**Abstract:** An ab initio study of proton-induced cleavage of $\alpha$ and $\beta$ glycopyranosides has been carried out at the 6-31G* level using protonated axial and equatorial methoxytetrahydropyran as models. The conformational changes along the reaction pathway can be monitored by focusing on the $C_5O_5$–$C_1C_2$ dihedral angle, $\omega$, which is +60° in the $^4C_1$ chair, and −60° in the $^{1,4}B$ boat. We have obtained the energy profiles of each protonated anomer for values of $\omega$ from −60° to +60°, and used these to select the most probable species that will proceed to the transition state. On the basis of least motion considerations, species in which $\omega$ = 0° are chosen on geometric grounds since the cleavage product, the cyclic oxocarbenium ion, is planar in the $C_5O_5$–$C_1C_2$ region. Additionally, low-energy conformers are considered possible precursors on the basis of energetic considerations. Stretching of the $C_1$–$O_1$ bonds of the plausible candidates then leads to the transition state. With respect to the cyclic oxocarbenium ion, a $\omega$ = 0° angle can be accommodated by several conformers, and the geometries and energies of these were evaluated. For the protonated axial anomer, the preferred intermediates are a flattened chair ($\omega$ = +37°), the $^0S_2$ boat, and the $E_3$ endo sofa. The first and third proceed to a half-chair transition state and thence to a half-chair oxocarbenium ion. The second proceeds to a transition state and oxocarbenium ion having $B_{2,5}$ boat structure and is found to be less favorable on the basis of energetic considerations. For the protonated equatorial anomer, the favored intermediates all proceed to a $^4E$ endo sofa transition state, and thence to an oxocarbenium ion of the same geometry. Thus, the $\alpha$ and $\beta$ anomers of the glycopyranosides are hydrolyzed through different retinues of intermediates and transition-state structures, and proceed to different cyclic oxocarbenium ions.

## Introduction

Replacement reactions at the anomeric center (e.g., **1** → **6**) are critical events in a wide variety of biological and chemical processes, and hence they have been subjected to extensive mechanistic investigations.[3] The substrates of greatest interest are oligosaccharides, and these are comprised (mainly) of glycopyranosidic residues. Since these glycosides, e.g., **1**, are acetals and therefore acid sensitive, mechanistic investigations have traditionally employed acid-catalyzed procedures,[4] and the weight of evidence is that protonation occurs on the exocyclic oxygen,[5,6] thereby triggering formation of the cyclic oxocarbenium ion (**1** → **2** → **3**, Scheme I).

Our recent discovery that *n*-pentenyl glycosides, e.g., **5**, could be "oxidatively hydrolyzed"[9] enabled us to gain access to the key intermediate **3** under neutral conditions. This capability paved the way for us to gain insight into the stereoelectronic requirements for glycoside cleavage and establish,[10] inter alia, that intermediate $^{1,4}B$ boat conformations were specifically excluded. These results prompted us to undertake[11] an ab initio study of acetal protonation based on the simplest member of that functional class, dimethoxymethane (**7**). This study revealed that protonation evokes profound changes in the geometric and energy relationships of various acetal conformations. For example, antiperiplanar *and* synperiplanar relationships between a lone pair and the protonated aglycon were *both* found to be stabilizing.[12]

**Scheme I**

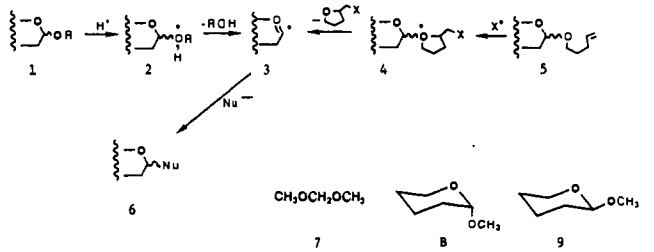


[†] Duke University.
[‡] University of North Carolina at Chapel Hill.

(1) This work was supported by grants from the National Science Foundation to B.F.-R. (CHE 8703916 and UTE 89 20033).
(2) (a) Taken from the Ph.D. Thesis of C.W.A., Duke University, 1989. Present address: Burroughs Wellcome Company, 3030 Cornwallis Road, Research Triangle Park, NC 27709. (b) Current address: Department of Chemistry, University of Georgia, Athens, GA 30602.
(3) For recent reviews, see: Sinnott, M. L. *Adv. Phys. Org. Chem.* **1988**, *24*, 113. Kirby, A. J. *Acc. Chem. Res.* **1985**, *17*, 305.
(4) Capon, B. *Chem. Rev.* **1969**, *69*, 40.
(5) Cleavage of glycosides is believed to occur via specific acid catalysis, indicating that the glycoside–proton bond is fully formed in the transition state. Bunton, C. A.; Lewis, T. A.; Llewellyn, D. R.; Vernon, C. A. *J. Chem. Soc.* **1955**, 4419. Banks, B. E. C.; Meinwald, Y.; Rhind-Tutt, A. J.; Sheft, L.; Vernon, C. A. *J. Chem. Soc.* **1961**, 3240.

0002-7863/91/1513-8293$02.50/0 